Fatigue Crack Propagation in Microcapsule Toughened Epoxy*

E. N. Brown[1,2,3], S. R. White[4,2], and N. R. Sottos[1,2]

[1]Department of Theoretical and Applied Mechanics
University of Illinois at Urbana-Champaign, Urbana, IL, 61801
[2]Beckman Institute for Advanced Science and Technology
University of Illinois at Urbana-Champaign, Urbana, IL, 61801
[3]Present Address: Materials Science and Technology Division
Los Alamos National Laboratory, Los Alamos, NM, 87545
[4]Department of Aerospace Engineering
University of Illinois at Urbana-Champaign, Urbana, IL, 61801

Abstract

The addition of liquid-filled urea-formaldehyde (UF) microcapsules to an epoxy matrix leads to significant reduction in fatigue crack growth rate and corresponding increase in fatigue life. Mode-I fatigue crack propagation is measured using a tapered double-cantilever beam (TDCB) specimen for a range of microcapsule concentrations and sizes: 0, 5, 10, and 20% by weight and 50, 180, and 460 μm diameter. Cyclic crack growth in both the neat epoxy and epoxy filled with microcapsules obeys the Paris power law. Above a transition value of the applied stress intensity factor ΔK_T, which corresponds to loading conditions where the size of the plastic zone approaches the size of the embedded microcapsules, the Paris law exponent decreases with increasing content of microcapsules, ranging from 9.7 for neat epoxy to approximately 4.5 for concentrations above 10 wt% microcapsules. Improved resistance to fatigue crack propagation, indicated by both the decreased crack growth rates and increased cyclic stress intensity for the onset of unstable fatigue-crack growth, is attributed to toughening mechanisms induced by the embedded microcapsules as well as crack shielding due to the release of fluid as the capsules are ruptured. In addition to increasing the inherent fatigue life of epoxy, embedded microcapsules filled with an appropriate healing agent provide a potential mechanism for self-healing of fatigue damage.

Keywords: fatigue-crack propagation, microcapsule toughening, tapered double-cantilevered beam, brittle fracture of epoxy

* Submitted for publication in *Journal of Materials Science* (2004) LANL LAUR-04-2668

1. Introduction

Highly crosslinked epoxy resins have low strain-to-failure and exhibit poor resistance to crack propagation. Fatigue loading is particularly problematic, causing small cracks to initiate and grow rapidly. These cracks often lead to catastrophic failure. An extensive body of work exists for the general area of fatigue of polymers [1–3], which focuses on understanding the mechanisms of fatigue and predicting the rates of fatigue-crack growth.

Fatigue crack propagation studies are performed with the cyclic-crack-tip stress state varying over a range defined by $\Delta K_I \equiv (K_{max} - K_{min})$. Dependence of the fatigue-crack-growth rate da/dN on the applied range of stress intensity factors ΔK_I is generally described by the empirical Paris law equation [4]

$$\frac{da}{dN} = C_0 \Delta K_I^n , \tag{1}$$

where C_0 and n are material constants that depend on the ratio of applied stress intensity $R \equiv K_{min}/K_{max}$, the loading frequency f, and the testing environment. The typical crack growth behavior described by Eq. (1) yields a linear log–log plot that is bounded by a threshold stress intensity range ΔK_{th} below which a crack ceases to propagate, and the critical stress intensity K_{IC} above which crack growth in unstable.

Several researchers [5–7] have successfully measured fatigue-crack propagation in epoxy resins and obtained values of the Paris law exponent n on the order of 10. Incorporation of either a rubbery second phase [8–11] or solid particles [7,12–13] significantly improves the resistance to fatigue-crack propagation. Several of these studies [5,8–9,11,13–14] suggest that improvements in the resistance to fatigue crack propagation behavior are also associated with increased toughness in monotonic fracture [1–2,14–15].

Previously, we investigated the effect of embedded urea-formaldehyde (UF) microcapsules on the monotonic fracture properties of a self-healing epoxy [15]. In addition to providing an efficient mechanism for self-healing [16–18], the presence of liquid-filled microcapsules increased the virgin monotonic-fracture toughness of epoxy by up to 127% [15,17]. The increased toughening was correlated with a change in the fracture plane morphology from mirror-like to hackle markings with subsurface microcracking. The inherent fracture toughness as well as the healing efficiency both depended strongly on the size and concentration of microcapsules. In the current work, we extend this investigation to examine the influence of microcapsules on the fatigue crack propagation behavior of epoxy, with the effects of self-healing precluded. Consistent with the monotonic fracture studies, the addition of microcapsules to an epoxy matrix significantly increased the resistance to crack growth under dynamic loading conditions.

2. Experimental procedure

2.1. Materials and sample preparation

Urea-formaldehyde microcapsules containing dicyclopentadiene (DCPD) monomer were manufactured with average diameters of 50, 180, and 460 μm using the emulsion *in situ* polymerization microencapsulation method outlined by Brown *et al.* [19]. Shell wall thickness was 190 ± 30 nm for all batches. Tapered double-cantilever beam specimens

were cast from EPON® 828 epoxy resin (DGEBA) and 12 pph Ancamine® DETA (diethylenetriamine) curing agent with a prescribed concentration of microcapsules mixed into the resin. The epoxy mixture was degassed, poured into a closed silicone rubber mold and cured for 24 hours at room temperature, followed by 24 hours at 30° C. Relevant physical and mechanical properties of the microcapsules and neat epoxy are listed in Table 1. The tensile modulus and mode I critical stress intensity factor, K_{IC}, of the microcapsule toughened epoxy were measured as a function of capsule concentration by Brown *et al*. [15, 20] and Rzeszutko *et al*. [21] and summarized in Table 2.

TABLE 1 Properties of the constituent materials [15]

Properties	Epoxy	Urea-formaldehyde microcapsules
Density (kg/m^3)	1160	~1000
Diameter (μm)	—	50±20
		180±40
		460±80
Wall thickness (nm)	—	190±30
K_{IC} (MPa m$^{1/2}$)	0.55±0.04	—
Young's modulus (GPa)	3.4±0.1	—
Ultimate stress (MPa)	39±4	—

TABLE 2 Mechanical properties of neat epoxy and epoxy with embedded microcapsules [15]

Microcapsule concentration (wt%)	Diameter, d (μm)	Young's modulus, E (GPa)	Critical stress intensity factor, K_{IC} (MPa m$^{1/2}$)	Critical strain energy release rate, G_C (J/m^2)
0	—	3.4±0.1	0.55±0.04	88±14
5	50±20	3.2±0.1	1.1±0.1	350±70
10	50±20	—	1.2±0.2	—
20	50±20	—	1.1±0.1	—
5	180±40	3.2±0.1	0.78±0.16	190±90
10	180±40	2.8±0.1	1.2±0.2	430±170
20	180±40	2.7±0.1	1.0±0.2	400±130
10	460±80	—	0.92±0.07	—
20	460±80	—	1.2±0.1	—

2.2 Mechanical testing

The fatigue-crack propagation behavior of the microcapsule-modified epoxy was investigated using the tapered double-cantilever beam (TDCB) specimen shown in Fig. 1. Side grooves ensured controlled crack growth along the centerline of the brittle specimen. The TDCB geometry, developed by Mostovoy *et al*. [22], provided a crack-length-independent relationship between applied stress intensity factor K_I and load P,

$$K_I = \alpha P, \tag{2}$$

which only required knowledge of the coefficient α. For the TDCB sample geometry in Fig. 1, α = 11.2x10^3 m$^{-3/2}$ was determined experimentally [17]. A constant range of Mode-I stress intensity factor ΔK_I was achieved by applying a constant range of load ΔP, independent of crack length. The constant-K region of the TDCB specimen enables crack-growth-rate measurements over a range of cycles, rather than requiring use of the modified secant formulation commonly employed for changing ΔK_I of a compact tension specimen [14]. Moreover, the constant-K region is of great importance for observing the time-dependent effects of self-healing during growth of a fatigue-crack [20].

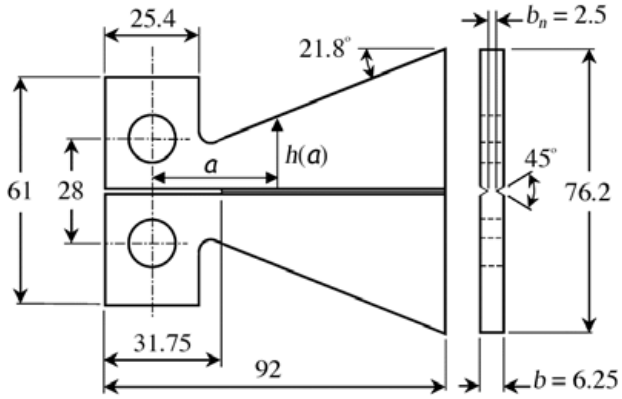

Figure 1. Tapered-double-cantilever-beam geometry [17]. All dimensions in mm.

Fatigue crack propagation studies were performed using an Instron DynoMight 8841 low-load frame with 250 N load-cell. Samples were precracked with a razor blade while ensuring the precrack tip was centered in the groove and then pin loaded. A triangular frequency of 5 Hz was applied with a load ratio ($R = K_{min}/K_{max}$) of 0.1. Crack lengths were determined by optical measurements at finite times and by compliance-inferred measurements [23] acquired approximately every 256th cycle.

The optically measured crack-tip position and specimen compliance are plotted against number of cycles in Fig. 2a. The linear relationship between optically measured crack length and specimen compliance (Fig. 2b) is used to calculate the crack-tip position at all times during the experiment (Fig. 2c). Crack-growth data are generated under constant ΔP (*i.e.* constant ΔK_I), with a complete set of loading conditions measured on a single specimen by incrementally increasing ΔP. Crack-growth rates are obtained from the number of cycles N required to grow a crack a distance Δa of approximately 1 mm for a given range of Mode-I stress intensity factor ΔK_I. Statistically equivalent values of crack-growth rate are obtain from using either the optically measured crack length prior to, $a_{i=0}^{opt}$, and following, $a_{i=S}^{opt}$, the application of N cycles at a give ΔK_I,

$$\left.\frac{da}{dN}\right|_{\Delta K} = \frac{\Delta a}{\Delta N} = \frac{a_{i=S}^{opt} - a_{i=0}^{opt}}{N_{i=S}}, \tag{3}$$

or from using a linear fit of the compliance-inferred measurements a_i^{comp},

$$\left.\frac{\mathrm{d}a}{\mathrm{d}N}\right|_{\Delta K} = \frac{S\sum_{i=1}^{S} N_i a_i^{\mathrm{comp}} - \sum_{i=1}^{S} N_i \sum_{i=1}^{S} a_i^{\mathrm{comp}}}{S\sum_{i=1}^{S} N_i^2 - \left(\sum_{i=1}^{S} N_i\right)^2}, \tag{4}$$

where S is the total number of cycle samples acquired.

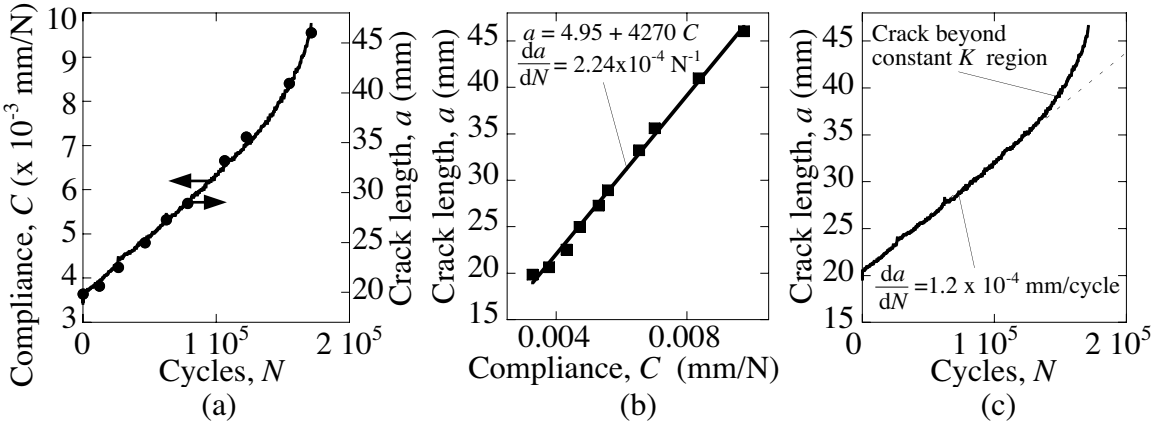

Figure 2. Plots illustrating method to calculate the continuous crack-tip position from compliance data (–) and finite optical measurements (●) (a). (b) Linear fit of optically measured crack *vs*. specimen compliance. The squares (■) represent compliance values corresponding to the optical data and the line (–) represents the linear best fit. (c) Crack length calculated from measured compliance using the relationship obtained from (b) plotted *vs*. number of cycles. The specimen is neat epoxy; the test parameters are $f = 5$ Hz, $R = 0.1$, and $\Delta K_{\mathrm{I}} = 0.472$ MPa m$^{1/2}$.

Fracture surface morphologies of the fatigue samples were examined with an environmental scanning electron microscope (Philips XL30 ESEM-FEG). After failure, specimens were mounted and sputtered with gold/palladium. Micrographs were obtained using 10kV secondary electrons in high vacuum mode.

3. Results

The effect of embedded microcapsule concentration on fatigue crack growth is shown in Fig. 3 for 180 μm diameter microcapsules. The relationship between the crack growth rate da/dN of epoxy and the applied range of Mode-I stress intensity factor ΔK_{I} clearly follows the Paris power law (Eq. 1). The measured Paris exponent is $n = 9.7$ for crack propagation in neat EPON® 828–Ancamine® DETA (no microcapsules). At applied stress intensity factors greater than $\Delta K \sim 0.35$ to 0.4 MPa m$^{1/2}$, a distinct transition in crack growth is observed for the microcapsule filled epoxy. Above a transition value ΔK_{T}, epoxy with microcapsules exhibits a higher resistance to fatigue crack growth than neat epoxy, accompanied by a reduction of the Paris law exponent n. At applied load levels below the transition point, the microcapsules have little influence on the crack growth rate.

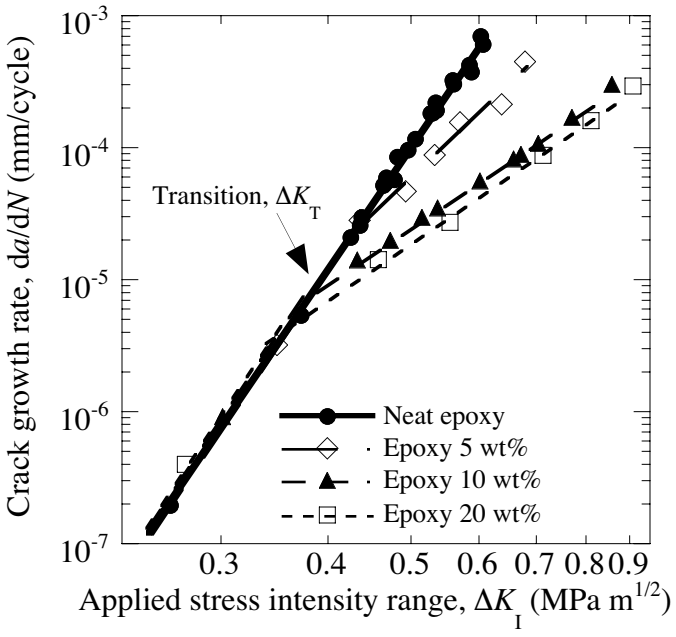

Figure 3. Influence of microcapsule concentration on the fatigue crack growth behavior for 180 μm diameter microcapsules.

Measured Paris law parameters for epoxy with embedded 50, 180, and 460 μm diameter microcapsules are summarized in Table 3. The Paris law exponent, n is plotted as a function of microcapsule concentration in Fig. 4. Above ΔK_T, the value of n decreases significantly with increasing microcapsule concentration, independent of capsule diameter. For concentrations greater than 10 wt% microcapsules, n has a steady-state value of approximately 4.5. Others have observed similar behavior for rubber-modified epoxies [14, 24].

TABLE 3 Constants of the Paris power law, ΔK_I^{max}, ΔK_T, and r_y

Microcapsule concentration (wt%)	Diameter (μm)	C_o (above ΔK_T)	n	ΔK_I^{max} (MPa m$^{1/2}$)	ΔK_T (MPa m$^{1/2}$)
0	—	8.2×10^{-2}	9.7	0.60	—
10	50±20	1.5×10^{-3}	4.9	0.82	0.41
20	50±20	1.6×10^{-3}	4.6	0.81	0.44
5	180±40	4.2×10^{-3}	6.1	0.64	0.46
10	180±40	5.4×10^{-4}	4.4	0.82	0.40
20	180±40	3.8×10^{-4}	4.3	0.80	0.36
10	460±80	7.8×10^{-4}	4.4	0.64	0.40
20	460±80	8.6×10^{-4}	4.7	0.82	0.39

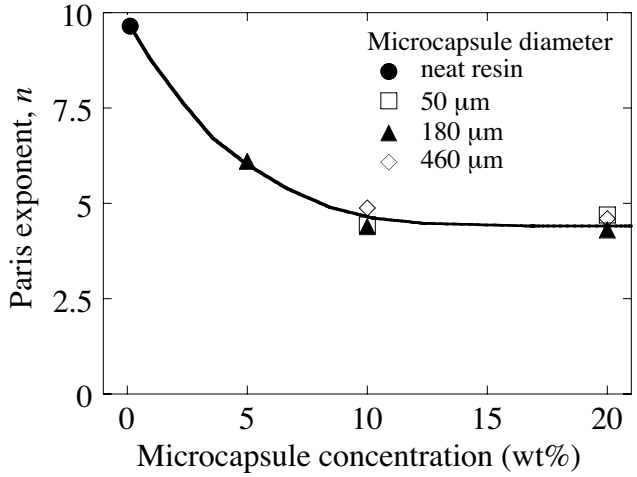

Figure 4. Influence of microcapsule concentration on Paris law exponent, n.

The effect of the microcapsules on life extension is shown more clearly in Fig. 5 by comparison of crack length as a function of loading cycles for neat epoxy and epoxy with 20 wt% microcapsules above ΔK_T. The addition of microcapsules significantly increases fatigue life; for the loading condition of $\Delta K_I = 0.586$ MPa m$^{1/2}$ the fatigue life increases from 86×10^3 cycles for neat epoxy to 239×10^3 for the microcapsule filled system.

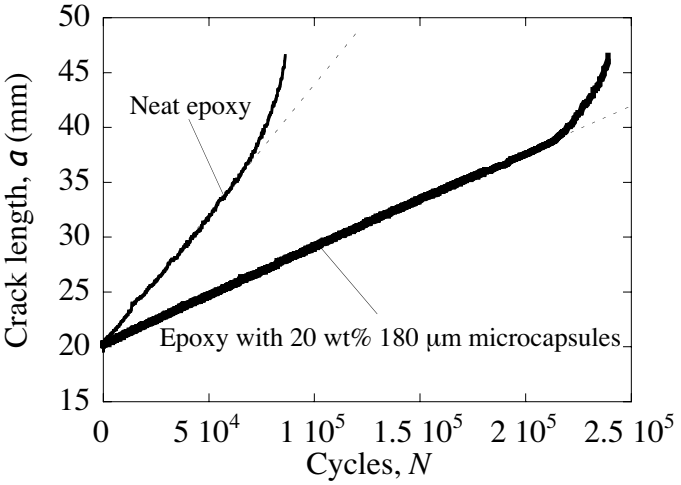

Figure 5. Fatigue crack extension *vs*. number of cycles for neat epoxy and epoxy with 20 wt% 180 microcapsules. The test parameters are $f = 5$ Hz, $R = 0.1$, and $\Delta K_I = 0.586$ MPa m$^{1/2}$.

Examination of the fatigue-fracture surface for neat epoxy reveals a relatively featureless morphology (Fig. 6a–c). River markings [25] are observed on some fracture surfaces, but are only initiated at locations corresponding to the crack-tip position when ΔK_I is incrementally increased (Fig. 6d–f). In contrast, the fatigue-fracture surface for epoxy with embedded microcapsules is characterized by substantial out-of-plane morphology at all length scales (Fig. 7). At the largest length scale, the microcapsules are ruptured at the fracture plane (similar to monotonic fracture), the fatigue-crack-growth path has significant deviation in and out of the plane, and the crack branches out of the plane at several locations (Fig. 7a). At smaller length scales the microcapsule walls have numerous secondary cracks (Fig. 7b,c) and the matrix has additional contortion and river markings at decreasing length scales (Fig. 7d,e).

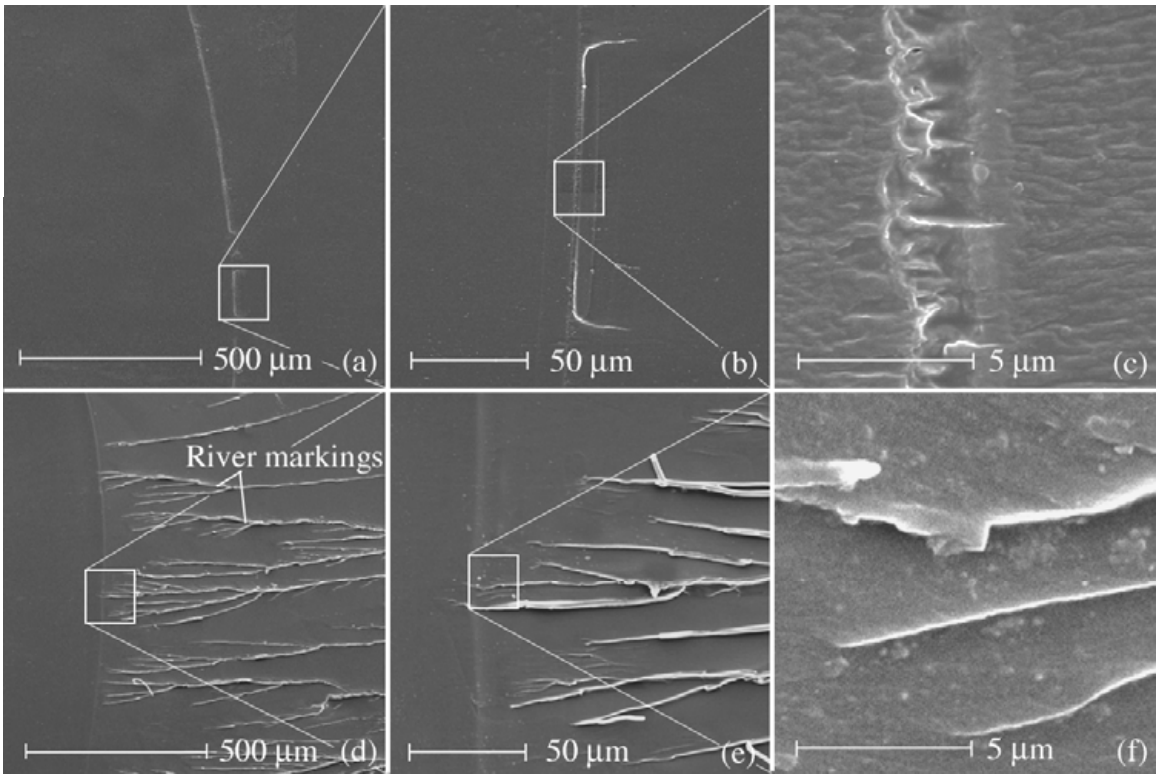

Figure 6. Fatigue-fracture surfaces for neat epoxy. (a–c) The dominant surface morphology is featureless at different length scales and (d–f) has some local river markings. Note: The crack propagation is from left to right in all images.

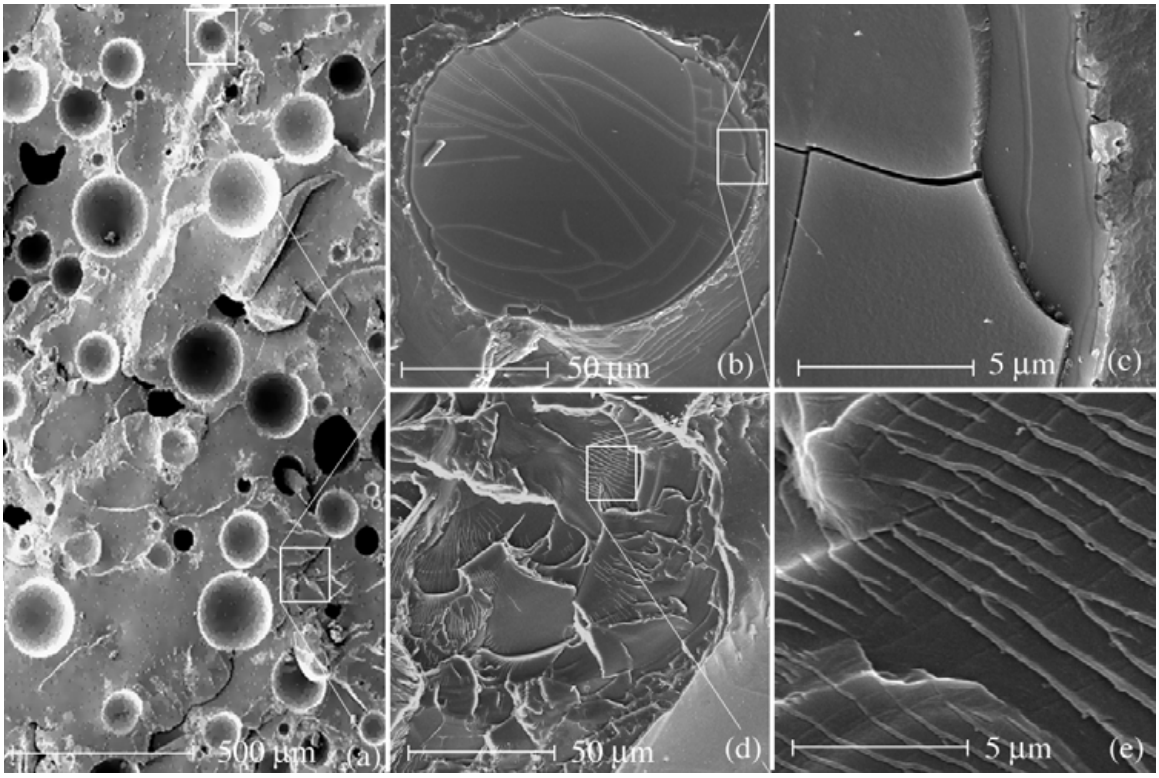

Figure 7. Fatigue-fracture surfaces for epoxy with 20 wt% of 180 µm microcapsules. (a) At large length scales the fracture plane has a contorted crack-growth path and ruptured microcapsules. At smaller length scales (b,c) the microcapsules exhibit cracking and (d,e) the matrix has complex morphology. Note: The crack propagation is from left to right in all images.

4. Discussion

The addition of microcapsules significantly improves the fatigue response above a transition value of the applied stress intensity factor, ΔK_T. Similar improvements reported in the literature for rubber modified epoxies have been explained by effects of plastic zone size [11,14] and increases of monotonic fracture toughness [5,8–9,11,13–14]. Azimi *et al.* [12,14] observed a transition point in the fatigue crack propagation behavior of DGEBA epoxies modified with CTBN and silicon rubber. Above a threshold value, the rubber-modified epoxy exhibited improved resistance to fatigue crack growth. Below the threshold, both neat epoxy and the rubber-modified epoxy had similar resistance. The transition was attributed to interactions between the rubber particles and the plastic zone present at the crack tip. Moreover, Azimi showed that the transition phenomenon was triggered when the size of the theoretical crack-tip plastic zone was of the order of the size of the filler.

Applying Azimi's hypothesis [12,14] to microcapsule-toughened epoxy, the theoretical plastic zone size at a cyclically loaded crack tip is estimated based on Irwin's [26] formula for the size of a plastic zone,

$$r_y(\Delta K_T) = \frac{1}{2\pi}\left(\frac{\Delta K_T/(1-R)}{\sigma_{YS}}\right)^2, \quad (5)$$

where σ_{YS} is the yield stress of the epoxy with embedded microcapsules. In previous work, Irwin's formula accurately captured the plastic zone size in EPON® 828–Ancamine® DETA under monotonic fracture conditions [15]. The plastic zone size estimated by Eq. (5) for 5, 10, and 20 wt% of 180 μm diameter microcapsules is c.a. 70 μm (assuming σ_{YS} = 20 MPa [15]). The calculated plastic zone size at the transition point for samples with 180 μm is within an order of magnitude of the microcapsule diameter consistent with Azimi's findings for 2–3 μm diameter rubber particles. When ΔK_I is less than ΔK_T, the plastic zone is smaller than the embedded microcapsules. In this regime the plastic zone is unaffected by the microcapsules—other than the presence of discontinuities along the crack front—resulting in little or no toughening and a fatigue response similar to that of the neat epoxy. When ΔK_I is greater than ΔK_T, the plastic zone is sufficiently large to encompass the majority of microcapsules in its path, activating toughening mechanisms similar to those observed for monotonic fracture.

The onset of fatigue crack growth instability is generally considered to be equivalent to monotonic fracture. Hence, the maximum stress intensity value during the cycle when the fatigue crack propagation becomes unstable should correlate with the monotonic fracture toughness,

$$K_{max}\left(\Delta K_I^{max}\right) \equiv \frac{\Delta K_I^{max}}{1-R} = K_{IC} \quad (6)$$

In Fig. 8, ΔK_I^{max} values from Table 3 are plotted against the corresponding K_{IC} values from Table 2 for the range of microcapsule sizes and concentrations tested. With the exception of neat epoxy, the data for microcapsule filled epoxy falls close to a line with a slope less than unity ($K_{IC} > K_{max}(\Delta K_I^{max})$), indicating a trend of increasing fatigue crack growth resistance with increasing monotonic fracture toughness. A similar trend has been reported previously for rubber-modified epoxies [5,8–9,13], implying that the failure mechanisms for static fracture and fatigue failure in modified epoxies are comparable.

For neat epoxy the $K_{max}(\Delta K_I^{max})$ value at fatigue crack instability exceeds the static fracture toughness values K_{IC}. This anomalous behavior has been reported previously for other filled polymer systems [5,11–12,14]. The inconsistency between $K_{max}(\Delta K_I^{max})$ and K_{IC} is explained by differences in the crack-tip geometry [27] and to a lesser degree the loading rate [5,28] between monotonic and fatigue testing. Montonic fracture toughness values are determined using precracks generated by a razor blade as prescribed in ASTM Standard D 5045. In contrast, the maximum stress intensity values K_{max} are determined for a crack tip generated in fatigue by progressively increasing ΔK_I. As described by Xiao *et al*. [27], yielding and damage at the crack tip under cyclic loading can cause apparent fracture toughness values for DGEBA epoxy with precracks generated by fatigue to exceed fracture toughness values measured in samples with razor blade generated precracks by as much as 31%. Hence, the high value of ΔK_I^{max} for neat epoxy is an artifact of the specimen loading history introducing progressive blunting at

the crack tip. This effect was only observed in the neat epoxy and is not present in the microcapsule modified systems.

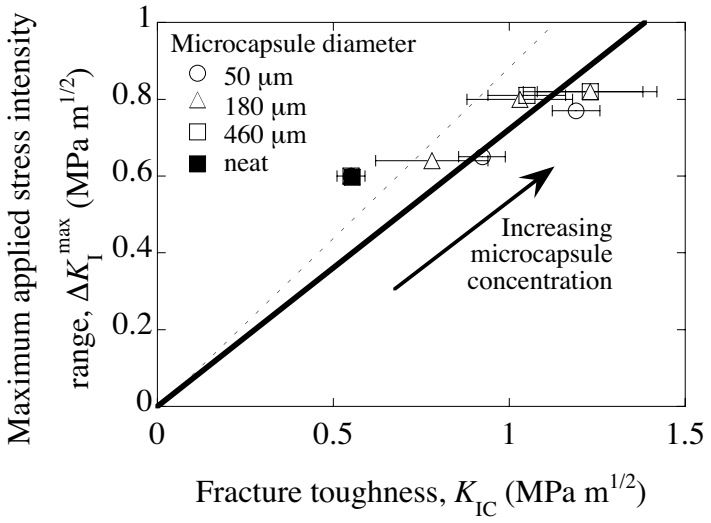

Figure 8. Influence of K_{IC} on ΔK_I^{max}. The dashed line corresponds to the maximum applied stress intensity range ΔK_I^{max} for fatigue crack instability when $K_{max}(\Delta K_I^{max}) \equiv \Delta K_I^{max}/(1\text{-}R) = K_{IC}$. The solid line is the best linear fit through the data points and the origin.

In addition to the toughening mechanisms induced by the embedded microcapsules, the flow of fluid released into the crack plane provides a crack tip shielding mechanism that can improve resistance to fatigue crack propagation. Several authors have reported that hydrodynamic pressure due to viscous flow within a fatigue crack reduces the effective range of Mode-I stress intensity and hence the fatigue crack growth rate for metal submerged in oil [29–32]. During cyclic loading, the crack volume changes significantly with time, requiring fluid flow into and out of the crack. When the crack contains a viscous fluid, the forces required to squeeze the fluid out of the crack during unloading and draw fluid into the crack during loading can be sufficient to shield the crack tip. Reduced crack growth rates in epoxy due to crack tip shielding from viscous fluid flow have been demonstrated for infiltration of both precatalyzed dicyclopentadiene and mineral oil [20].

5. Conclusions

Fatigue crack propagation was investigated in epoxy toughened with liquid-filled urea-formaldehyde (UF) microcapsules. The addition of microcapsules significantly decreased the fatigue crack growth rate and increased the fatigue life above a transition value of the stress intensity factor ΔK_T. Below ΔK_T the fatigue behavior was unaffected by the embedded microcapsules. The transition value between these two regimes corresponded to loading conditions where the size of the plastic zone approached the size of the embedded microcapsules. The fatigue-crack growth rate dependence on applied range of stress intensity ΔK_I was accurately captured by the Paris power law in both neat epoxy and epoxy with embedded microcapsules. The Paris law exponent *n*

was strongly dependent on the microcapsule concentration, varying from 9.7 for neat epoxy to approximately 4.5 above 10 wt% microcapsules, but was independent of microcapsule diameter. The onset of unstable fatigue-crack growth ΔK_I^{max} increased with monotonic fracture toughness, and was independent of microcapsule diameter. Improved resistance to fatigue crack propagation, was attributed to toughening mechanisms induced by the embedded microcapsules as evidenced by changes in the fatigue fracture plane morphology. In addition to increasing the inherent fatigue life of epoxy, embedded microcapsules filled with an appropriate healing agent offer a potential mechanism to further extend fatigue life through self-healing of fatigue damage.

Acknowledgments

The authors gratefully acknowledge support from the AFOSR Aerospace and Materials Science Directorate Mechanics and Materials Program (Award No. F49620-00-1-0094), the National Science Foundation (NSF CMS0218863), and Motorola Labs, Motorola Advanced Technology Center, Schaumburg Ill. Any opinions, findings, and conclusions or recommendations expressed in this publication are those of the authors and do not necessarily reflect the views of the AFOSR or Motorola Labs. The authors would also like to thank Profs. J.S. Moore and P.H. Geubelle of the Autonomic Materials Laboratory of the Beckman Institute of Advanced Science and Technology and Dr. A. Skipor of Motorola Labs for technical support and helpful discussions. Electron microscopy was performed in the Imaging Technology Group, Beckman Institute, of the University of Illinois at Urbana-Champaign, with the assistance of S. Robinson.

References

1. R. J. CARDOSO, A. SHUKLA, and A. BOSE, *J. Mater. Sci.* **37** (2002) 603.
2. R. BAGHERI and R. A. PEARSON, *J. Mater. Sci.* **31** (1996) 4529.
3. M. D. SKIBO, R. W. HERTZBERG, J. A. MANSON, and S. L. KIM, *J. Mater. Sci.* **12** (1977) 531.
4. P. C. PARIS, M. P. GOMEZ, and W. E. ANDERSON, *The Trend in Engineering at the University of Washington* **13** (1961) 9.
5. J. KARGER-KOCSIS and K. FRIEDRICH, *Compos. Sci. Technol.* **48** (1993) 263.
6. M. NAGASAWA, H. KINUHATA, H. KOIZUKA, K. MIYAMOTO, T. TANAKA, H. KISHIMOTO, and T. KOIKE, *J. Mater. Sci.* **30** (1995) 1266.
7. M. K. McMURRAY and S. AMAGI, *J. Mater. Sci.* **34** (1999) 5927.
8. L. BECU, A. MAAZOUZ, H. SAUTEREAU, and J. F. Gerard, *J. Appl. Polym. Sci.* **65** (1997) 2419.
9. L. REY, N. POISSON, A. MAAZOUZ, and H. SAUTEREAU, *J. Mater. Sci.* **34** (1999) 1775.
10. B. S. HAYES and J. C. SEFERIS, *Polym. Compos.* **22** (2001) 451.
11. H. R. AZIMI, R. A. PEARSON, and R. W. HERTZBERG, *Polym. Eng. Sci.* **36** (1996) 2352.
12. H. R. AZIMI, R. A. PEARSON, and R. W. HERTZBERG, *J. Appl. Polym. Sci.* **58** (1995) 449.
13. H. SAUTEREAU, A. MAAZOUZ, J. F. GERARD, and J. P. TROTIGNON, *J. Mater. Sci.* **30** (1995) 1715.
14. H. R. AZIMI, R. A. PEARSON, and R. W. HERTZBERG, *J. Mater. Sci.* **31**

(1996) 3777.
15. E. N. BROWN, S. R. WHITE, and N. R. SOTTOS, *J. Mater. Sci.* **39** (2004) 1703.
16. S. R. WHITE, N. R. SOTTOS, P. H. GEUBELLE, J. S. MOORE, M. R. KESSLER, S. R. SRIRAM, E. N. BROWN, and S. VISWANATHAN, *Nature* **409** (2001) 794.
17. E. N. BROWN, N. R. SOTTOS, and S. R. WHITE, *Exp. Mech.* **42** (2002) 372.
18. M. R. KESSLER, N. R. SOTTOS, and S. R. WHITE, *Composites Part A* **34** (2003) 743.
19. E. N. BROWN, M. R. KESSLER, N. R. SOTTOS, and S. R. WHITE, *J. Microencapsul.* **20** (2003) 719.
20. E. N. BROWN, in "Fracture and Fatigue of a self-healing polymer composite material" (PhD dissertation, University of Illinois at Urbana-Champaign) (2003) p. 103.
21. A. A. RZESZUTKO, E. N. BROWN, and N. R. SOTTOS, *2003 Proc. 5th Undergraduate Research Conf. in Mechanics* (*University of Illinois at Urbana-Champaign, TAM Report No. 1041*) (2004) 27.
22. S. MOSTOVOY, P. B. CROSLEY, and E.J. RIPLING, *J. Materials* **2** (1967) 661.
23. A. SAXENA and S. J. HUDAK Jr., *Int. J. Fract.* **14** (1978) 453.
24. J. KARGER-KOCSIS and K. FRIEDRICH, *Colloid Polym. Sci.* **270** (1992) 549.
25. A. CHUDNOVSKY, A. KIM, and C. P. BOSNYAK, *Int. J. Fract.* **55** (1992) 209.
26. G. R. IRWIN, *Proc. 7th Sagamore Ornance Mater. Res. Conf.* **4** (1960) 63.
27. K. XIAO, L. YE, and Y. S. KWOK, *J. Mater. Sci.* **33** (1998) 2831.
28. W. ARAKI, T. ADACHI, M. GAMOU, and A. YAMAJI, *Proc. I. Mech. E. Part L* **216** (2002) 79.
29. K.ENDO, T. OKADA, K. KOMAI, and M. KIYOTA, *Bull. Japan Soc. Mech. Eng.* **15** (1972) 1316.
30. G. GALVIN, and H. NAYLOR, *Proc. Inst. Mech. Eng. J* **179** (1964) 56.
31. W.J. PLUMBRIDGE, P.J. ROSS, and J.S.C. PARRY, *Mater. Sci. Eng.* **68** (1985) 219.
32. C. POLK, W. MURPHY, and C. ROWE, *ASLE Transactions* **18** (1975) 290.

List of Recent TAM Reports

No.	Authors	Title	Date
962	Harris, J. G.	Rayleigh wave propagation in curved waveguides—*Wave Motion* **36**, 425–441 (2002)	Jan. 2001
963	Dong, F., A. T. Hsui, and D. N. Riahi	A stability analysis and some numerical computations for thermal convection with a variable buoyancy factor—*Journal of Theoretical and Applied Mechanics* **2**, 19–46 (2002)	Jan. 2001
964	Phillips, W. R. C.	Langmuir circulations beneath growing or decaying surface waves—*Journal of Fluid Mechanics* (submitted)	Jan. 2001
965	Bdzil, J. B., D. S. Stewart, and T. L. Jackson	Program burn algorithms based on detonation shock dynamics—*Journal of Computational Physics* (submitted)	Jan. 2001
966	Bagchi, P., and S. Balachandar	Linearly varying ambient flow past a sphere at finite Reynolds number: Part 2—Equation of motion—*Journal of Fluid Mechanics* **481**, 105–148 (2003) (with change in title)	Feb. 2001
967	Cermelli, P., and E. Fried	The evolution equation for a disclination in a nematic fluid—*Proceedings of the Royal Society A* **458**, 1–20 (2002)	Apr. 2001
968	Riahi, D. N.	Effects of rotation on convection in a porous layer during alloy solidification—Chapter 12 in *Transport Phenomena in Porous Media* (D. B. Ingham and I. Pop, eds.), 316–340 (2002)	Apr. 2001
969	Damljanovic, V., and R. L. Weaver	Elastic waves in cylindrical waveguides of arbitrary cross section—*Journal of Sound and Vibration* (submitted)	May 2001
970	Gioia, G., and A. M. Cuitiño	Two-phase densification of cohesive granular aggregates—*Physical Review Letters* **88**, 204302 (2002) (in extended form and with added co-authors S. Zheng and T. Uribe)	May 2001
971	Subramanian, S. J., and P. Sofronis	Calculation of a constitutive potential for isostatic powder compaction—*International Journal of Mechanical Sciences* (submitted)	June 2001
972	Sofronis, P., and I. M. Robertson	Atomistic scale experimental observations and micromechanical/continuum models for the effect of hydrogen on the mechanical behavior of metals—*Philosophical Magazine* (submitted)	June 2001
973	Pushkin, D. O., and H. Aref	Self-similarity theory of stationary coagulation—*Physics of Fluids* **14**, 694–703 (2002)	July 2001
974	Lian, L., and N. R. Sottos	Stress effects in ferroelectric thin films—*Journal of the Mechanics and Physics of Solids* (submitted)	Aug. 2001
975	Fried, E., and R. E. Todres	Prediction of disclinations in nematic elastomers—*Proceedings of the National Academy of Sciences* **98**, 14773–14777 (2001)	Aug. 2001
976	Fried, E., and V. A. Korchagin	Striping of nematic elastomers—*International Journal of Solids and Structures* **39**, 3451–3467 (2002)	Aug. 2001
977	Riahi, D. N.	On nonlinear convection in mushy layers: Part I. Oscillatory modes of convection—*Journal of Fluid Mechanics* **467**, 331–359 (2002)	Sept. 2001
978	Sofronis, P., I. M. Robertson, Y. Liang, D. F. Teter, and N. Aravas	Recent advances in the study of hydrogen embrittlement at the University of Illinois—Invited paper, Hydrogen–Corrosion Deformation Interactions (Sept. 16–21, 2001, Jackson Lake Lodge, Wyo.)	Sept. 2001
979	Fried, E., M. E. Gurtin, and K. Hutter	A void-based description of compaction and segregation in flowing granular materials—*Continuum Mechanics and Thermodynamics*, in press (2003)	Sept. 2001
980	Adrian, R. J., S. Balachandar, and Z.-C. Liu	Spanwise growth of vortex structure in wall turbulence—*Korean Society of Mechanical Engineers International Journal* **15**, 1741–1749 (2001)	Sept. 2001
981	Adrian, R. J.	Information and the study of turbulence and complex flow—*Japanese Society of Mechanical Engineers Journal B*, in press (2002)	Oct. 2001
982	Adrian, R. J., and Z.-C. Liu	Observation of vortex packets in direct numerical simulation of fully turbulent channel flow—*Journal of Visualization*, in press (2002)	Oct. 2001
983	Fried, E., and R. E. Todres	Disclinated states in nematic elastomers—*Journal of the Mechanics and Physics of Solids* **50**, 2691–2716 (2002)	Oct. 2001
984	Stewart, D. S.	Towards the miniaturization of explosive technology—Proceedings of the 23rd International Conference on Shock Waves (2001)	Oct. 2001

List of Recent TAM Reports (cont'd)

No.	*Authors*	*Title*	*Date*
985	Kasimov, A. R., and Stewart, D. S.	Spinning instability of gaseous detonations—*Journal of Fluid Mechanics* (submitted)	Oct. 2001
986	Brown, E. N., N. R. Sottos, and S. R. White	Fracture testing of a self-healing polymer composite—*Experimental Mechanics* (submitted)	Nov. 2001
987	Phillips, W. R. C.	Langmuir circulations—*Surface Waves* (J. C. R. Hunt and S. Sajjadi, eds.), in press (2002)	Nov. 2001
988	Gioia, G., and F. A. Bombardelli	Scaling and similarity in rough channel flows—*Physical Review Letters* **88**, 014501 (2002)	Nov. 2001
989	Riahi, D. N.	On stationary and oscillatory modes of flow instabilities in a rotating porous layer during alloy solidification—*Journal of Porous Media* **6**, 1–11 (2003)	Nov. 2001
990	Okhuysen, B. S., and D. N. Riahi	Effect of Coriolis force on instabilities of liquid and mushy regions during alloy solidification—*Physics of Fluids* (submitted)	Dec. 2001
991	Christensen, K. T., and R. J. Adrian	Measurement of instantaneous Eulerian acceleration fields by particle-image accelerometry: Method and accuracy—*Experimental Fluids* (submitted)	Dec. 2001
992	Liu, M., and K. J. Hsia	Interfacial cracks between piezoelectric and elastic materials under in-plane electric loading—*Journal of the Mechanics and Physics of Solids* **51**, 921–944 (2003)	Dec. 2001
993	Panat, R. P., S. Zhang, and K. J. Hsia	Bond coat surface rumpling in thermal barrier coatings—*Acta Materialia* **51**, 239–249 (2003)	Jan. 2002
994	Aref, H.	A transformation of the point vortex equations—*Physics of Fluids* **14**, 2395–2401 (2002)	Jan. 2002
995	Saif, M. T. A, S. Zhang, A. Haque, and K. J. Hsia	Effect of native Al_2O_3 on the elastic response of nanoscale aluminum films—*Acta Materialia* **50**, 2779–2786 (2002)	Jan. 2002
996	Fried, E., and M. E. Gurtin	A nonequilibrium theory of epitaxial growth that accounts for surface stress and surface diffusion—*Journal of the Mechanics and Physics of Solids* **51**, 487–517 (2003)	Jan. 2002
997	Aref, H.	The development of chaotic advection—*Physics of Fluids* **14**, 1315–1325 (2002); see also *Virtual Journal of Nanoscale Science and Technology*, 11 March 2002	Jan. 2002
998	Christensen, K. T., and R. J. Adrian	The velocity and acceleration signatures of small-scale vortices in turbulent channel flow—*Journal of Turbulence*, in press (2002)	Jan. 2002
999	Riahi, D. N.	Flow instabilities in a horizontal dendrite layer rotating about an inclined axis—*Journal of Porous Media*, in press (2003)	Feb. 2002
1000	Kessler, M. R., and S. R. White	Cure kinetics of ring-opening metathesis polymerization of dicyclopentadiene—*Journal of Polymer Science A* **40**, 2373–2383 (2002)	Feb. 2002
1001	Dolbow, J. E., E. Fried, and A. Q. Shen	Point defects in nematic gels: The case for hedgehogs—*Proceedings of the National Academy of Sciences* (submitted)	Feb. 2002
1002	Riahi, D. N.	Nonlinear steady convection in rotating mushy layers—*Journal of Fluid Mechanics* **485**, 279–306 (2003)	Mar. 2002
1003	Carlson, D. E., E. Fried, and S. Sellers	The totality of soft-states in a neo-classical nematic elastomer—*Journal of Elasticity* **69**, 169–180 (2003) with revised title	Mar. 2002
1004	Fried, E., and R. E. Todres	Normal-stress differences and the detection of disclinations in nematic elastomers—*Journal of Polymer Science B: Polymer Physics* **40**, 2098–2106 (2002)	June 2002
1005	Fried, E., and B. C. Roy	Gravity-induced segregation of cohesionless granular mixtures—*Lecture Notes in Mechanics*, in press (2002)	July 2002
1006	Tomkins, C. D., and R. J. Adrian	Spanwise structure and scale growth in turbulent boundary layers—*Journal of Fluid Mechanics* (submitted)	Aug. 2002
1007	Riahi, D. N.	On nonlinear convection in mushy layers: Part 2. Mixed oscillatory and stationary modes of convection—*Journal of Fluid Mechanics* (submitted)	Sept. 2002

List of Recent TAM Reports (cont'd)

No.	*Authors*	*Title*	*Date*
1008	Aref, H., P. K. Newton, M. A. Stremler, T. Tokieda, and D. L. Vainchtein	Vortex crystals—*Advances in Applied Mathematics* **39**, in press (2002)	Oct. 2002
1009	Bagchi, P., and S. Balachandar	Effect of turbulence on the drag and lift of a particle—*Physics of Fluids*, in press (2003)	Oct. 2002
1010	Zhang, S., R. Panat, and K. J. Hsia	Influence of surface morphology on the adhesive strength of aluminum/epoxy interfaces—*Journal of Adhesion Science and Technology* **17**, 1685–1711 (2003)	Oct. 2002
1011	Carlson, D. E., E. Fried, and D. A. Tortorelli	On internal constraints in continuum mechanics—*Journal of Elasticity* **70**, 101–109 (2003)	Oct. 2002
1012	Boyland, P. L., M. A. Stremler, and H. Aref	Topological fluid mechanics of point vortex motions—*Physica D* **175**, 69–95 (2002)	Oct. 2002
1013	Bhattacharjee, P., and D. N. Riahi	Computational studies of the effect of rotation on convection during protein crystallization—*International Journal of Mathematical Sciences*, in press (2004)	Feb. 2003
1014	Brown, E. N., M. R. Kessler, N. R. Sottos, and S. R. White	*In situ* poly(urea-formaldehyde) microencapsulation of dicyclopentadiene—*Journal of Microencapsulation* (submitted)	Feb. 2003
1015	Brown, E. N., S. R. White, and N. R. Sottos	Microcapsule induced toughening in a self-healing polymer composite—*Journal of Materials Science* (submitted)	Feb. 2003
1016	Kuznetsov, I. R., and D. S. Stewart	Burning rate of energetic materials with thermal expansion—*Combustion and Flame* (submitted)	Mar. 2003
1017	Dolbow, J., E. Fried, and H. Ji	Chemically induced swelling of hydrogels—*Journal of the Mechanics and Physics of Solids*, in press (2003)	Mar. 2003
1018	Costello, G. A.	Mechanics of wire rope—Mordica Lecture, Interwire 2003, Wire Association International, Atlanta, Georgia, May 12, 2003	Mar. 2003
1019	Wang, J., N. R. Sottos, and R. L. Weaver	Thin film adhesion measurement by laser induced stress waves—*Journal of the Mechanics and Physics of Solids* (submitted)	Apr. 2003
1020	Bhattacharjee, P., and D. N. Riahi	Effect of rotation on surface tension driven flow during protein crystallization—*Microgravity Science and Technology* **14**, 36–44 (2003)	Apr. 2003
1021	Fried, E.	The configurational and standard force balances are not always statements of a single law—*Proceedings of the Royal Society* (submitted)	Apr. 2003
1022	Panat, R. P., and K. J. Hsia	Experimental investigation of the bond coat rumpling instability under isothermal and cyclic thermal histories in thermal barrier systems—*Proceedings of the Royal Society of London A*, in press (2003)	May 2003
1023	Fried, E., and M. E. Gurtin	A unified treatment of evolving interfaces accounting for small deformations and atomic transport: grain-boundaries, phase transitions, epitaxy—*Advances in Applied Mechanics*, in press (2003)	May 2003
1024	Dong, F., D. N. Riahi, and A. T. Hsui	On similarity waves in compacting media—*Horizons in Physics*, in press (2003)	May 2003
1025	Liu, M., and K. J. Hsia	Locking of electric field induced non-180° domain switching and phase transition in ferroelectric materials upon cyclic electric fatigue—*Applied Physics Letters*, in press (2003)	May 2003
1026	Liu, M., K. J. Hsia, and M. Sardela Jr.	In situ X-ray diffraction study of electric field induced domain switching and phase transition in PZT-5H—*Journal of the American Ceramics Society* (submitted)	May 2003
1027	Riahi, D. N.	On flow of binary alloys during crystal growth—*Recent Research Development in Crystal Growth*, in press (2003)	May 2003
1028	Riahi, D. N.	On fluid dynamics during crystallization—*Recent Research Development in Fluid Dynamics*, in press (2003)	July 2003

List of Recent TAM Reports (cont'd)

No.	*Authors*	*Title*	*Date*
1029	Fried, E., V. Korchagin, and R. E. Todres	Biaxial disclinated states in nematic elastomers—*Journal of Chemical Physics* **119**, 13170–13179 (2003)	July 2003
1030	Sharp, K. V., and R. J. Adrian	Transition from laminar to turbulent flow in liquid filled microtubes—*Physics of Fluids* (submitted)	July 2003
1031	Yoon, H. S., D. F. Hill, S. Balachandar, R. J. Adrian, and M. Y. Ha	Reynolds number scaling of flow in a Rushton turbine stirred tank: Part I—Mean flow, circular jet and tip vortex scaling—*Chemical Engineering Science* (submitted)	Aug. 2003
1032	Raju, R., S. Balachandar, D. F. Hill, and R. J. Adrian	Reynolds number scaling of flow in a Rushton turbine stirred tank: Part II—Eigen-decomposition of fluctuation—*Chemical Engineering Science* (submitted)	Aug. 2003
1033	Hill, K. M., G. Gioia, and V. V. Tota	Structure and kinematics in dense free-surface granular flow—*Physical Review Letters*, in press (2003)	Aug. 2003
1034	Fried, E., and S. Sellers	Free-energy density functions for nematic elastomers—*Journal of the Mechanics and Physics of Solids*, in press (2003)	Sept. 2003
1035	Kasimov, A. R., and D. S. Stewart	On the dynamics of self-sustained one-dimensional detonations: A numerical study in the shock-attached frame—*Physics of Fluids* (submitted)	Nov. 2003
1036	Fried, E., and B. C. Roy	Disclinations in a homogeneously deformed nematic elastomer—*Nature Materials* (submitted)	Nov. 2003
1037	Fried, E., and M. E. Gurtin	The unifying nature of the configurational force balance—*Mechanics of Material Forces* (P. Steinmann and G. A. Maugin, eds.), in press (2003)	Dec. 2003
1038	Panat, R., K. J. Hsia, and J. W. Oldham	Rumpling instability in thermal barrier systems under isothermal conditions in vacuum—*Philosophical Magazine* (submitted)	Dec. 2003
1039	Cermelli, P., E. Fried, and M. E. Gurtin	Sharp-interface nematic–isotropic phase transitions without flow—*Archive for Rational Mechanics and Analysis* (submitted)	Dec. 2003
1040	Yoo, S., and D. S. Stewart	A hybrid level-set method in two and three dimensions for modeling detonation and combustion problems in complex geometries—*Combustion Theory and Modeling* (submitted)	Feb. 2004
1041	Dienberg, C. E., S. E. Ott-Monsivais, J. L. Ranchero, A. A. Rzeszutko, and C. L. Winter	Proceedings of the Fifth Annual Research Conference in Mechanics (April 2003), TAM Department, UIUC (E. N. Brown, ed.)	Feb. 2004
1042	Kasimov, A. R., and D. S. Stewart	Asymptotic theory of ignition and failure of self-sustained detonations—*Journal of Fluid Mechanics* (submitted)	Feb. 2004
1043	Kasimov, A. R., and D. S. Stewart	Theory of direct initiation of gaseous detonations and comparison with experiment—*Proceedings of the Combustion Institute* (submitted)	Mar. 2004
1044	Panat, R., K. J. Hsia, and D. G. Cahill	Evolution of surface waviness in thin films via volume and surface diffusion—*Journal of Applied Physics* (submitted)	Mar. 2004
1045	Riahi, D. N.	Steady and oscillatory flow in a mushy layer—*Current Topics in Crystal Growth Research* (submitted)	Mar. 2004
1046	Riahi, D. N.	Modeling flows in protein crystal growth—*Current Topics in Crystal Growth Research* (submitted)	Mar. 2004
1047	Bagchi, P., and S. Balachandar	Response of the wake of an isolated particle to isotropic turbulent cross-flow—*Journal of Fluid Mechanics* (submitted)	Mar. 2004
1048	Brown, E. N., S. R. White, and N. R. Sottos	Fatigue crack propagation in microcapsule toughened epoxy—*Journal of Materials Science* (submitted)	Apr. 2004